# VOLCANIC PARTICLES IN THE STRATOSPHERE

By Beverley Harris*

[*Manuscript received August* 11, 1964]

*Summary*

Measurements of intensities of sunlight reflected from a balloon during sunset indicate an above-average concentration of dust at stratospheric levels. Our results for May 1964 (combined with the results obtained by CSIRO from direct sampling of particles from aircraft) may be explained by the presence at 20-km altitude over Victoria of concentrations of the order of either (i) 500 000 metallic Aitken nuclei per litre, or (ii) a few thousand large aerosols per litre of the types observed in aircraft collections, but with thick coatings of dielectric material, or by the presence of both (i) and (ii).

## Introduction

Many investigators (Hogg 1963; Meinel and Meinel 1964; Volz 1964) have attributed recent colourful sunsets and increased atmospheric opacity to the ejection, and subsequent widespread distribution, of particles from the eruption of Mount Agung (latitude 10° S.) in Indonesia on March 17, 1963. Particles collected from a U-2 aircraft at 20-km altitude between 20° S. and 45° S. have been identified as of volcanic origin by Mossop (1963, 1964).

In the present paper we report on measurements of relative intensities of direct sunlight after reflection from a balloon levelled above the stratosphere (Fig. 1) by the method of Pittock (1963). Monochromatic measurements provide an estimate of the height of the intervening stratospheric dust. One set of observations made with two wavelengths, both unaffected by ozone, enables the extinction due to dust to be found. Hence, with the aid of Mossop's results, possible particle concentrations and compositions are inferred.

## Results and Analyses

Figure 2 presents the observational results for the dates indicated. The intensity $I$ of a single wavelength ($0 \cdot 44\ \mu$) in arbitrary units is graphed against time after ground sunset, which is a function of the minimum altitude of the light ray reaching the balloon ($h_{\min}$ in Fig. 1).

The curve for March 12, 1963 is typical of those obtained before the Bali eruption on March 17, 1963. It shows that light intensity was detectable up to about 22 min after ground sunset. After this time, when $h_{\min}$ was less than 9 km, the tangential light ray became extinguished in the troposphere.

* Department of Physics (RAAF Academy), University of Melbourne.

On the other hand, on October 8, 9, and 16, 1963 and May 6, 1964 the signal was lost after about 13–16 min corresponding to values of $h_{\mathrm{min}}$ of 21, 24, 23, and 19 km respectively.

For a purely molecular, dust-free atmosphere, the intensity for a tangential light ray at stratospheric altitudes is expected to decrease approximately linearly with time (Rayleigh scattering). The results in Figure 2 therefore lead to the conclusion that the presence of dust becomes a *significant* factor at altitudes of 22, 25, 25, and 23 km respectively for the above dates.

That the intensity profile of May 7, 1963 does not differ greatly from those obtained prior to the Bali eruption appears, at first, to be inconsistent with the southward movement of 1° per day of the volcanic ejecta, as given by Mossop on the basis of commencement times of vivid sunsets at several latitudes. However, his

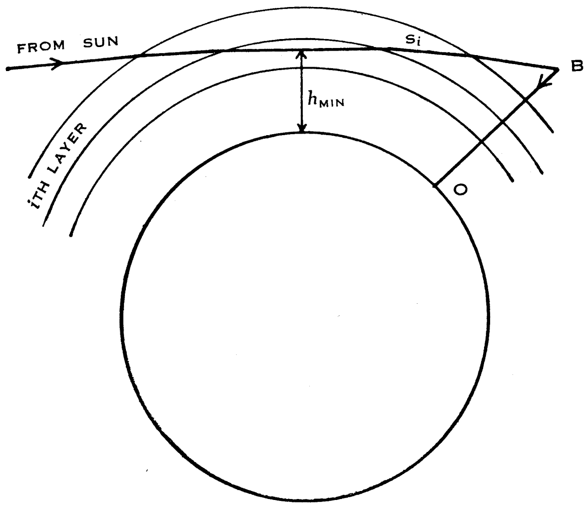


Fig. 1.—A section through the Earth containing the levelled balloon B, vertically above the observer at O (Melbourne, latitude 38° S.), and the path of sunlight traversing a distance $S_i$ in the $i$th layer in the stratosphere.

sampling results (Table 1 and Fig. 3) indicate an increasing proportion of smaller particles with increasing time after the eruption. These particles possibly had not arrived in the lower stratosphere over Victoria in quantities detectable by monochromatic measurements by May 1963.

For the twilight of May 6, 1964, intensity profiles were obtained for *two* wavelengths, $\lambda$ and $\lambda'$ (Fig. 4). From these curves one may find values of the left side of the equation

$$\frac{1}{I'}\frac{\mathrm{d}I'}{\mathrm{d}h_{\mathrm{min}}}-\left(\frac{\lambda}{\lambda'}\right)^4\frac{1}{I}\frac{\mathrm{d}I}{\mathrm{d}h_{\mathrm{min}}}=\sigma\sum_i N_i\frac{\mathrm{d}S_i}{\mathrm{d}h_{\mathrm{min}}}, \tag{1}$$

where, in the present case, primed and unprimed symbols refer to wavelengths of

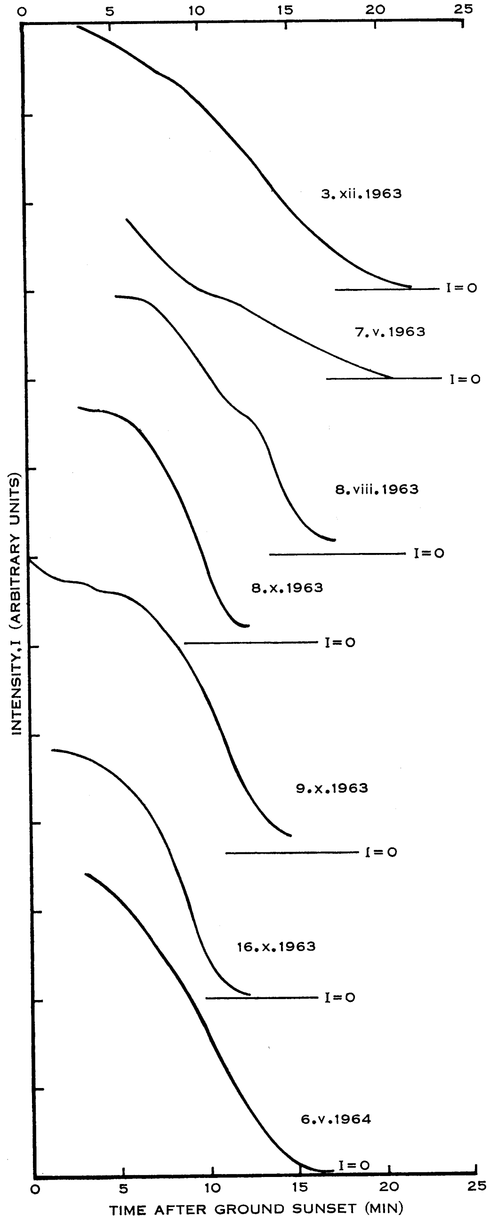


Fig. 2.—Some observed intensity profiles for $\lambda = 0 \cdot 44\ \mu$ for the dates indicated, without minor corrections for variation of the balloon–observer distance and magnification effect (the intensity scales are arbitrary).

$0 \cdot 44$ and $0 \cdot 70\ \mu$ respectively. This equation assumes that the aerosol is distributed with uniform number concentration $N_i$ in the $i$th layer.

TABLE 1

PARTICLE CONCENTRATIONS DERIVED FROM U-2 COLLECTIONS IN THE LOWER STRATOSPHERE*

| Date | Total Particle Concentration (per litre) | Volcanic Particles (per litre) | Ratio of Volcanic to Total Particle Concentration |
|---|---|---|---|
| Apr. 23, 1963 | 34 | 0·6 | 0·02 |
| May 7, 1963 | 160 | 31 | 0·19 |
| May 21, 1963 | 23 | 6·6 | 0·29 |
| July 3, 1963 | — | 88 | — |
| Dec. 3, 1963 | 400 | 38 | 0·1 |
| Apr. 2, 1964 | 400 | 32 | 0·1 |

* Supplied by Dr. Mossop.

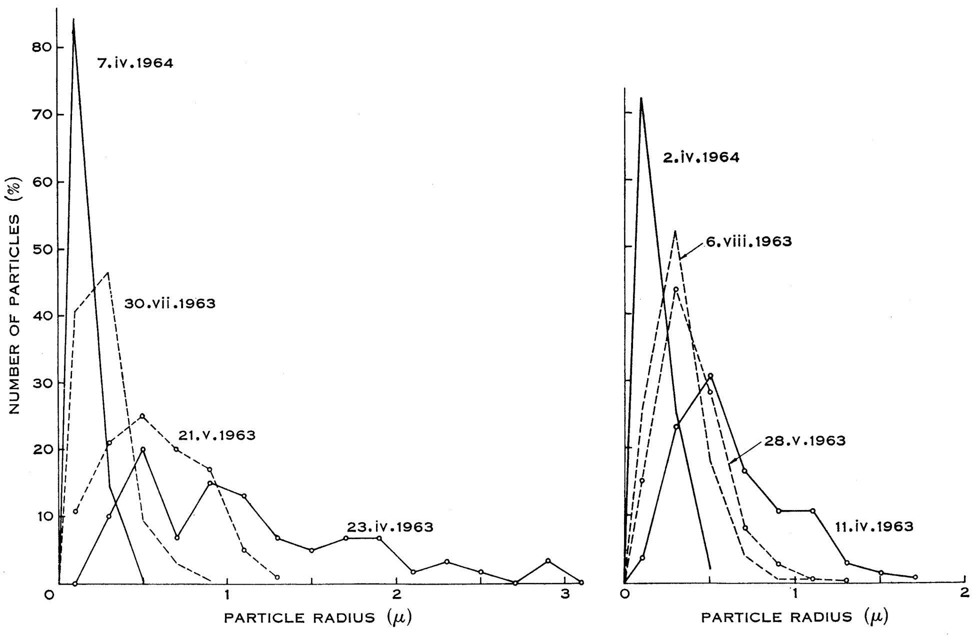


Fig. 3.—Size distributions of volcanic particles for the accompanying dates (supplied by Dr. Mossop).

For a given $h_{\min}$, $S_i$ is the corresponding light path length shown in Figure 1. $\sigma$ is given by

$$\sigma = \int_{r_2}^{r_1} \pi r^2 n(r) \{(\lambda/\lambda')^4 K(r/\lambda, m) - K(r/\lambda', m')\} \, \mathrm{d}r, \tag{2}$$

where $K(r/\lambda, m)$ is the Mie efficiency factor for extinction for a spherical particle of radius $r$ and refractive index $m$. The size distribution $n(r)$ must satisfy the relation

$$\int_{r_2}^{r_1} n(r)\,\mathrm{d}r = 1,$$

where $r_1$ and $r_2$ are the upper and lower radius limits of the distribution under consideration. $\sigma$ then may be determined uniquely from the parameters $m$, $n(r)$, $r_1$, and $r_2$ of a given aerosol model. Thus, various models are investigated, and the corresponding $N_i$ calculated from equation (1) by successive approximation.

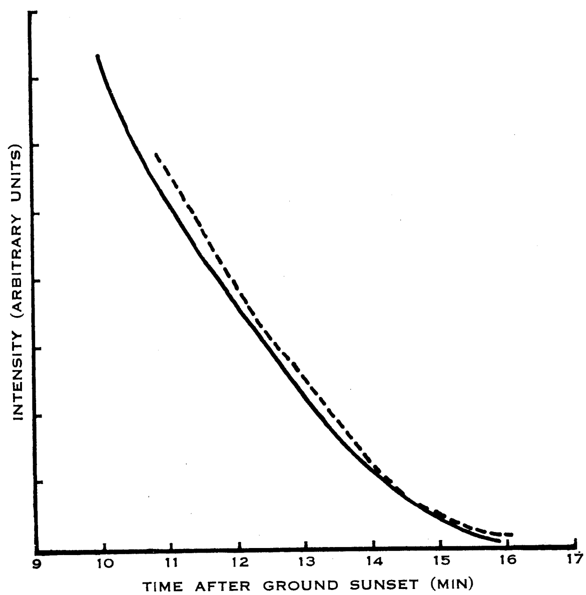


Fig. 4.—Intensity profiles obtained during sunset on May 6, 1964 for the wavelengths $0\cdot 44\,\mu$ (– – – –) and $0\cdot 70\,\mu$ (———), with the corrections mentioned under Figure 2.

Model A is chosen as representative of sampling results and the size distribution reported by Mossop for July 3, 1963 (Fig. 5, curve (*a*)). The lower limit is determined by the insensitivity of the twilight balloon method to particles of real refractive index and with radii less than $0\cdot 05\,\mu$. The values of $K(r/\lambda, m)$ tabulated by Penndorf (1956) are used in the numerical evaluation of the integral, with $m = m' = 1\cdot 40$, which is appropriate to the physical appearance and results of chemical analysis (Mossop 1963, 1964, and personal communication).

Model B assumes the size distribution of Figure 5, curve (*b*), with the same refractive index as for model A.

For model C, calculations were made assuming the major aerosol component to be particles of iron, too small to have been detectable by Mossop. Thus $m$ and $m'$ for this model were taken to be $1\cdot 27 - 1\cdot 37i$ and $1\cdot 80 - 2\cdot 00i$ respectively (Schalen 1939). Figure 5, curve (*c*) shows the model C size distribution.

According to the calculations of Junge, Chagnon, and Manson (1961) particles of radii less than $0 \cdot 01\ \mu$ are expected to be removed rapidly by coagulation, hence defining $r_2$. Mossop's most recent results (Fig. 3) indicate an increasing proportion of solid particles with radii below approximately $0 \cdot 1\ \mu$, which is therefore the value taken as the upper radius limit. The values of $K(r/\lambda, m)$ computed by Schalen (1939) were used in the evaluation of equation (2).

Model D approximates Mossop's results for April 7, 1964. It differs from model A in that the radii of insoluble particles are reduced by a factor of three. These particles are also assumed to have water-soluble coatings of refractive index $1 \cdot 4$, and thickness about nine times the core radii.

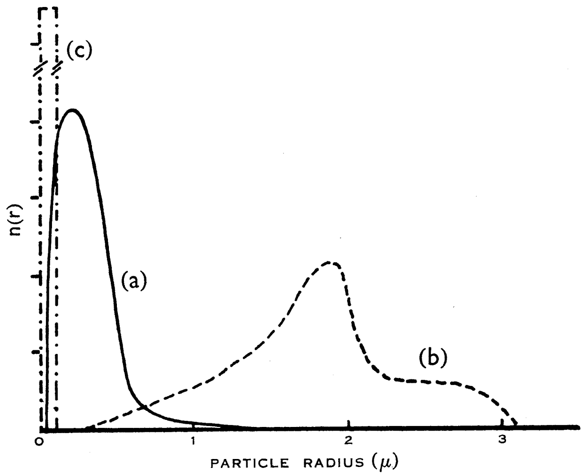


Fig. 5.—Size distributions of stratospheric particles (Mossop, personal communication) derived from (*a*) sampling results of July 3, 1963, (*b*) sampling results of April 23, 1963, and (*c*) the experimental and theoretical results of Junge, Chagnon, and Manson (1961).

## Conclusions

Table 2 summarizes the various model characteristics and lists the corresponding values of $N$, calculated for the 20-km level.

Models A and B result in concentrations too large to be consistent with the sampling data. Model C implies the existence of concentrations of the order of 500 000 *Aitken* nuclei per litre at 20 km; and model D shows the possibility of large coated particles of concentrations of about 3000 per litre.

The concentration–altitude profile in Figure 6, constructed assuming altitude independence of the model, shows that dust concentrations are decreasing above the lower height limit of the present technique (18–20 km). Meinel and Meinel (1964) estimated the mean apparent height of the dust layer from sunset measurements to be $17 \cdot 8$ km.

These results of optical probing and direct sampling techniques may be interpreted in two ways: (1) very high concentrations of metallic Aitken nuclei, (2) concentrations of a few thousand per litre of large aerosol particles of $0 \cdot 1$ to $1\ \mu$ radius, which have grown coatings of thicknesses several times their radius. (This latter possibility is supported by the work of Mossop (1964 and personal communications).) It is of course possible that a combination of both types existed at the 20-km level over Victoria during May 1964.

Adaption of the existing apparatus specifically for stratospheric aerosol detection will improve the reliability of future results.

TABLE 2

PARTICLE CONCENTRATIONS AT 20 KM FOR THE MODEL SIZE DISTRIBUTIONS SHOWN IN FIGURE 5

| Model | Size Distribution | $r_1$ ($\mu$) | $r_2$ ($\mu$) | $N$ (particles/litre) |
|---|---|---|---|---|
| A | Fig. 5, curve (*a*) | 1·5 | 0·05 | 35 000 |
| B | Fig. 5, curve (*b*) | 3·0 | 0·30 | 70 |
| C | Fig. 5, curve (*c*) | 0·10 | 0·01 | 500 000 |
| D | See text | 5·0 | 0·17 | 3 000 |

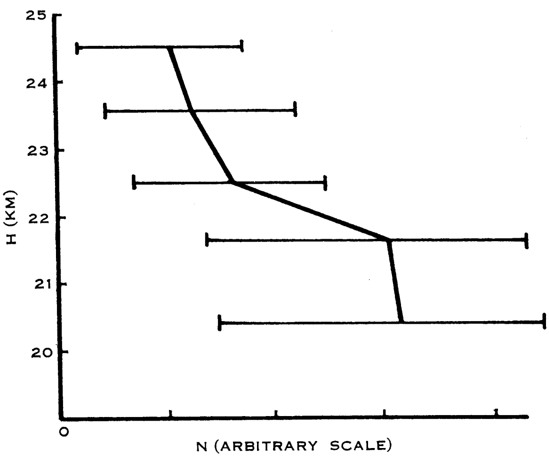


Fig. 6.—The altitude profile of particle number concentration for the twilight of May 6, 1964. The horizontal scale is linear but dependent on the model, as seen in Table 2.

## ACKNOWLEDGMENTS

The author is indebted to Dr. S. Mossop of the Division of Radiophysics, CSIRO, Sydney, for allowing the use of his unpublished data, and is also grateful to Professor Hopper and Mr. G. Paltridge for helpful discussions, and to many of the staff of the Physics Department (RAAF Academy), particularly Dr. Jean Laby, Mr. E. Unthank, Mr. J. Sparrow, and Mr. G. Martin, for assisting with the observations. This work was supported by a grant from the University of Melbourne and the Royal Australian Air Force.

## References


Hogg, A. R. (1963).—*Aust. J. Sci.* **26**(4): 119–20.

Junge, C. E., Chagnon, C. W., and Manson, J. E. (1961).—*J. Meteorol.* **18**: 81–108.

Meinel, A. B., and Meinel, M. P. (1964).—*Nature* **201**: 657–8.

Mossop, S. C. (1963).—*Nature* **199**: 325–6.

Mossop, S. C. (1964).—*Nature* (In press.)

Penndorf, R. B. (1956).—Geophysical Research Papers No. 45, Part 6 (ASTIA Document No. AD-98772).

Pittock, A. B. (1963).—*J. Geophys. Res.* **68**: 5143–55.

Schalen, C. (1939).—*Annlr. Uppsala Astr. Obs.* **1**, No. 2.

Volz, F. E. (1964).—*Science* **144**: 1121–2.